Available online at www.sciencedirect.com
ScienceDirect
C. R. Physique 10 (2009) 159–166
COMPTES RENDUS PHYSIQUE

Laser acceleration of particles in plasmas / Accélération laser de particules dans les plasmas

Quasi-monoenergetic electron acceleration in relativistic laser-plasmas

Alexander Pukhov [a,*], Sergei Gordienko [a], Vasili Seredov [a], Igor Kostyukov [b]

[a] *Institut für Theoretische Physik I, Heinrich-Heine-Universität, 40225 Düsseldorf, Germany*
[b] *Institut for Applied Physics RAS, Nizhni Novgorod, Russia*

Available online 25 April 2009

Abstract

Using Particle-in-Cell simulations as well as analytical theory we study electron acceleration in underdense plasmas both in the Bubble regime and in the weakly relativistic periodic wake fields. In the Bubble regime, electron trapping is taken as a function of the propagated distance. The number of trapped electrons depends on the effective phase velocity of the X-point at the rear of the Bubble. For the weakly relativistic periodic wakes, we show that the phase synchronism between the wake and the relativistic electrons can be maintained over very long distances when the plasma density is tapered properly. Moreover, one can use layered plasmas to control and improve the accelerated beam quality. ***To cite this article: A. Pukhov et al., C. R. Physique 10 (2009).***

Résumé

Accélération par laser d'électrons quasi-monoénergétiques dans les plasmas relativistes. A partir de simulations numériques et de théorie analytique, on étudie l'accélération d'électrons dans des plasmas sous-denses, à la fois dans le régime de la bulle et dans le régime du champ de sillage périodique faiblement relativiste. Dans le régime de la bulle le piégeage électronique est considéré comme une fonction de la distance de propagation. Le nombre d'électrons piégés dépend de la vitesse de phase effective du point X à l'arrière de la bulle. Dans le régime du champ de sillage périodique faiblement relativiste, on montre que la synchronisation de phase entre le sillage et les électrons relativistes peut être maintenu sur de longues distances à condition que la densité de plasma soit correctement profilée. De plus, on peut utiliser des couches de plasmas pour contrôler et améliorer la qualité du faisceau. ***Pour citer cet article : A. Pukhov et al., C. R. Physique 10 (2009).***

Keywords: Laser; Plasma; Acceleration

Mots-clés : Laser ; Plasma ; Accélération

1. Introduction

The maximum achievable laser powers have grow fast over the last ten years and have reached the Petawatt (10^{15} W) values in a single shot [1–3], and is projected to the Exawatt (10^{18} W) level in the near future. This enor-

* Corresponding author.
E-mail address: pukhov@tp1.uni-duesseldorf.de (A. Pukhov).

1631-0705/$ – see front matter
doi:10.1016/j.crhy.2009.03.013

mous power is comparable to that which the Sun sends to the Earth. Of course, these powerful laser pulses last for an extremely short time, just for a few femtoseconds (1 fs $= 10^{-15}$ s). It means that these laser pulses represent just a few cycles of radiation. It is this short pulse duration that allows for the extremely high power, while the energy remains in a reasonable range, from Joules to a few kiloJoules.

When focused, these laser pulses can produce fields of the order of TV/cm (10^{12} V/cm). Thus, one of the main applications for these ultra-intense laser pulses is the acceleration of charged particles. Unfortunately, the laser fields are oscillatory and transverse. A particle being accelerated by the laser fields directly, slips out of the acceleration phase very fast and the maximum energy gain is limited. One has to elaborate special accelerating schemes, like the Laser Wake Field Acceleration (LWFA) scheme [4] and Direct Laser Acceleration (DLA) at the betatron resonance [5].

A major breakthrough has been achieved with the invention of the so-called "Bubble" regime of LWFA [6]. The major advantage of the Bubble is the natural generation of quasi-monoenergetic electron beams. The first successful experiments in the Bubble regime were reported in 2004, where electron beams with energies in the range 70...170 MeV were observed [7–9]. By optimizing the interaction geometry and improving the laser parameters, nearly GeV energies of electron beams have been reached recently [10–12].

Up to now, there is no strict analytical model for the Bubble acceleration, although a few "phenomenological" models do exist [13,14]. Apart of these, we have developed the relativistic similarity theory [15] that allows us to scale the Bubble in a wide parameter range. On the basis of this theory we were able to show that the Bubble scalings are the optimal ones for electron acceleration in the relativistic limit of underdense plasmas, $S \to 0$ [16]. Here, $S = n/a_0 n_c$ is the relativistic similarity number, $a_0 = eA/mc^2$ is the relativistically normalized laser amplitude, $n_c = m\omega^2/4\pi e^2$ is the critical density for the laser with the carrier frequency ω.

Despite the success of the similarity theory, it remains unclear what is the reason for the mono-energeticity of the electron beam emerging from the Bubble and whether one can influence the beam quality in any way. In this work, we present some numerical studies on the electron trapping in the Bubble regime.

In contrast to the Bubble regime, the weakly relativistic periodic wake field is well described analytically [17]. Here, we discuss how a properly tapered plasma density profiles can be used to control the acceleration process and the beam quality [18].

2. Laser Wake Field Acceleration

When a laser pulse propagates through underdense plasmas, it excites a running plasma wave oscillating at the plasma frequency $\omega_p = \sqrt{4\pi n e^2/m}$, where n is the background electron density, e and m are the electron charge and mass, respectively. The wave trails the laser pulse with the phase velocity set by the laser pulse group velocity $v_{ph}^{wake} = v_g$. It is useful to introduce the relativistic γ-factor related to the pulse group velocity $\gamma_g = 1/\sqrt{1 - v_g^2/c^2}$. The electric field of the plasma wave is longitudinal, i.e., it points into the propagation direction. A relativistic electron can ride on this plasma wave staying in-phase with this longitudinal electric field over large distances and be accelerated to high energies.

The laser pulse can excite the plasma wave in different ways. The excitation is most effective when the laser pulse is shorter than the plasma wavelength, λ_p, and fits completely into the first wave bucket.

The length of the laser pulse is a parameter of particular significance. The pattern of wake field excitation differs significantly for laser pulses longer and shorter than the plasma period. The long laser pulse gets self-modulated with the plasma period, and the resonance between this self-modulation and the plasma frequency leads to effective wake field excitation. The corresponding regime of particle acceleration is called Self-Modulated Laser Wake Field Acceleration (SM-LWFA) [19–22] in contrast to the short-pulse LWFA described before.

To estimate the maximum energy gain of a relativistic electron in the laser wake field, one introduces the so-called dephasing length L_d. It defines how long the electron remains in the accelerating phase of the wake that makes roughly one half of λ_p. Lorentz transformations then lead to the expression $L_d = 0.5\gamma_g^2 \lambda_p$. Consequently, the maximum energy gain $W_{\max} = eE_{\max} L_d$, where $E_{\max}$ is the amplitude of the wake. Here we have supposed that the laser depletion length L_{depl} is longer than the dephasing length: $L_{depl} > L_d$.

To achieve high quality of the accelerated electron beam, one needs a perfectly synchronized external injector that can produce ultra-short electron bunches, much shorter than the plasma wavelength to occupy a small portion of the accelerating phase, where the electric field is nearly constant. Different schemes have been proposed to accomplish

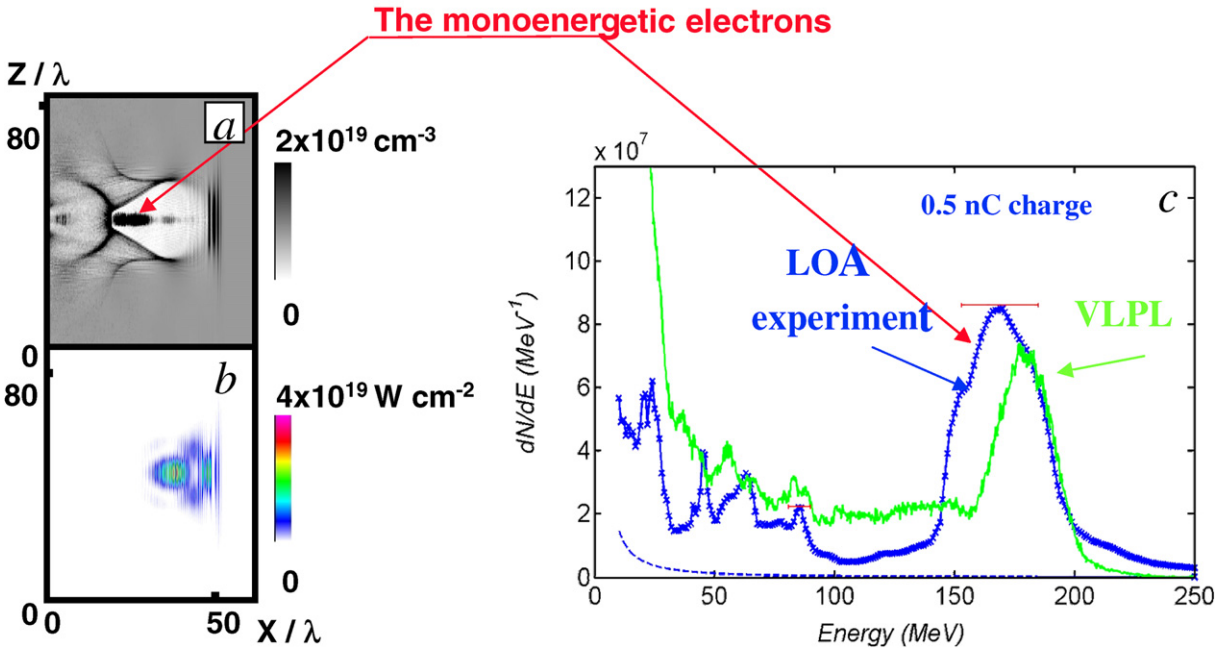

Fig. 1. 3D PIC simulations for the LOA experiment [9]. (a) On-axis cut of the electron density: the characteristic bubble structure and the trapped electron beam. (b) On-axis cut of the laser intensity. The laser pulse is self-focused and compressed. (c) Electron spectra measured in the experiment and the simulation.

the electron injection by all-optical means involving two or more laser pulses [23–25]. The most successful and experimentally working one has been implemented by the LOA group [26].

3. 3D regime of relativistic LWFA: the Bubble

The properties of laser wake fields can be well described analytically when the laser amplitude is not too high and the plasma wave is regular. However, when the electric field of a planar plasma wave reaches the limit $E_{wb}/E_0 = \sqrt{2(\gamma_p - 1)}$, where $\gamma_p = (1 - v_g^2/c^2)^{-1/2} = \omega_0/\omega_p$, the wave breaks [27]. The wave breaking is manifested in a multi-stream electron motion. The wave amplitude is so high that the oscillation velocity of electrons in the wave becomes comparable with the wave phase velocity. As a consequence, the background plasma electrons can catch the wave, be trapped in the wave potential and be accelerated. The wave breaking regime is extremely nonlinear and needs a kinetic description. What happens after the wave is broken, depends on the geometrical dimensionality of the wave breaking region. In the simplest 1d geometry, the breaking always happens in the first half plasma wave. In 2d and 3d geometries, the breaking depends on the strength of plasma wave excitation and other plasma conditions. It has been noticed by the authors of [28–31] that in the multi-dimensional relativistic regime the plasma wave fronts are curved. The wave breaks near the axis and for lower values of the electric field than the plane wave limit. Because the breaking region can occupy just a small portion of the wave around the axis, the large-scale structure of the wave may remain stable. The wave as a whole survives the breaking, and the trapped electrons can be accelerated over large distances and gain energy.

Wave breaking turns out to be of central importance because it leads to abundant self-trapping of electrons in the potential of the wave bucket which are then accelerated in large numbers. This results in a high conversion efficiency of laser energy into relativistic beam energy. Trapping of electrons in the plasma waves is a key topic for LWFA. At relativistic laser intensities, the wake field breaks after the very first period and mutates to a solitary cavity: the Bubble [6]. This is a highly relativistic regime and there are natural difficulties in its analytical description. Up to now, only phenomenological theories exist able to describe very general properties of the fields distribution in the Bubble [13]. A complete analytical model is still absent.

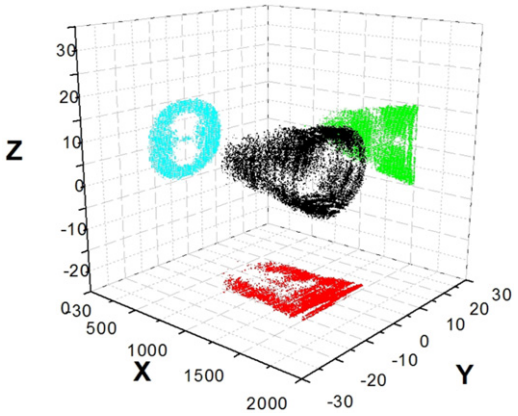

Fig. 2. Three-dimensional view of initial positions of particles, which have been trapped in the Bubble after 2 mm propagation distance.

At the same time, the relativistic similarity theory [15] allows us to write down simple scalings on the electron acceleration in the Bubble regime. It tells us that the Bubble regime is stable and scalable.

4. Reaching Bubble regime in experiments

As we mentioned above, the Bubble regime of electron acceleration and the resulted quasi-monoenergetic electron beams are now observed in a number of independent experiments. Here, we return once more to the LOA experiment [9], which has been simulated with the 3D PIC code VLPL. A comparison of the experimentally measured spectrum and the simulation is shown in Fig. 1. The quasi-monoenergetic electron beam has the energy 170 ± 20 MeV and the charge about 0.5 nC. Looking at the geometry of the laser wake field in the simulation, one can mention that the plasma wave behind the laser pulse starts to recall the characteristic bubble structure. Applying the formula for the threshold laser power needed to form a bubble [15], one obtains that the LOA experiment [9] has been done at the lowest bubble power threshold. One may expect that with upgraded laser power, the stability and quality of the electron beam will be further improved.

5. Electron trapping in the Bubble

The central question of the Bubble acceleration is: what is the reason for generation of the quasi-monoenergetic electron beam? To clarify this, we have followed trajectories of all trapped and accelerated electrons. Fig. 2 shows a 3D view of the initial positions of the trapped electrons. Apparently, the trapped electrons were located on a cylindrical surface, nearly corresponding to the Bubble radius. The process of electron trapping by an electron cavity moving at relativistic velocity has been discussed analytically in [13]. It has been shown there that a rather thin layer of plasma located at the Bubble radius exists, where electrons can be trapped. Electrons located closer to the laser axis pass through the Bubble, and those located farther away simply pass by. We see from Fig. 2 that at the very beginning of the interaction, the surface is slightly deformed and elongated in the polarization direction. At this stage, the Bubble was shorter than the laser pulse, and the laser field influenced the trapping process significantly. Later, the laser shortened and fitted the Bubble. This lead to a more round shape of the trapping surface.

Fig. 3(a) shows the number of electrons trapped as a function of propagated distance. Apparently, the trapping rate is not constant, but changes in time. There are regions in the plasma with a rather poor trapping interchanged with regions of quite intense trapping. To elucidate the question of what influences the trapping process, we plot the current position x of accelerated electrons in the Bubble vs their initial positions x_0 in the plasma, Fig. 3(b). The distribution of particles in this plot has a rather sharp upper boundary, that can be approximated by a curve. If we assume that the Bubble traps plasma electrons like a “snow plough”, then the current coordinates x represent the relativistically compressed original coordinate x_0 like

$$x \approx \frac{1}{4\gamma_X^2} x_0 \tag{1}$$

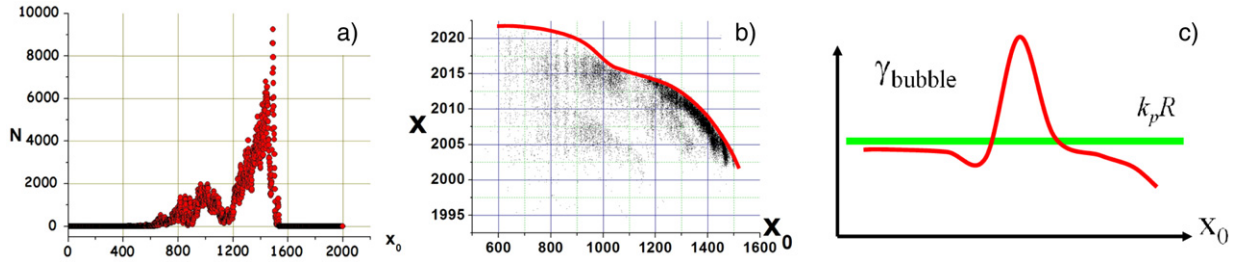

Fig. 3. (a) Number of trapped particles as a function of the propagation distance. We see that the trapping is highly non-uniform. There are regions in plasma, where the trapping was very efficient and regions, where trapping was absent at all. (b) Current coordinate x of electrons trapped in the Bubble vs their original coordinate x_0. The distribution has a sharp upper boundary marked by the line. This line is due to the "snow plough" relation (1). (c) Effective relativistic γ-factor of the trapping point in the Bubble as compared with the normalized Bubble radius $k_p R_{\text{bubble}}$ (horizontal line). The Bubble can trap electrons only if the condition (2) is satisfied.

where γ_X is the effective relativistic γ-factor of the trapping X-point in the Bubble. At the rear part of the electron bunch, $2002 < x/\lambda < 2015$, electrons do concentrate at this line. At the front of the bunch, electrons have a significant spread, most probably because they are interacting with the tail of the laser pulse here.

Using the snow plough relation (1), we can see how the effective γ_X evolves during the interaction. A qualitative estimate is given in Fig. 3(c). The horizontal line in Fig. 3(c) gives the normalized Bubble radius $k_p R_{\text{bubble}}$. According to the analytical theory [13], the Bubble can trap electrons only if its radius is larger than its γ-factor:

$$\gamma_X < k_p R_{\text{bubble}} \tag{2}$$

and the better the inequality (2) is satisfied, the more electrons can be trapped by the Bubble.

Apparently, at the very beginning of interaction, $600 < x_0/\lambda < 850$, γ_X was relatively high. The number of trapped electrons was not so high in this region. Then γ_X decreased and simultaneously the number of trapped electrons increased in the range $900 < x_0/\lambda < 1100$. Then, for some reason, γ_X grew drastically in the range $1100 < x_0/\lambda < 1200$, and the trapping nearly ceased here. At the end of interaction $x_0/\lambda > 1200$, the Bubble slowed down and the trapping intensified excessively.

This complicated dynamics highlights the highly nonlinear physics of the Bubble regime of acceleration. The oscillations of the trapping point velocity at the beginning of the interaction can be explained by the fact that the laser is oscillating around some attractor solution [15], because it is very difficult to match it initially. The slow down at the end is the consequence of the "beam loading" and simultaneously the laser depletion and frequency downshift. The beam loading leads to cavity elongation [6,13] and thus to the effective slowing down of the trapping point located at the rear of the cavity. These effects have to be studied further.

6. Control of laser wake field acceleration by plasma density profile

In this section we discuss particle acceleration in a low amplitude periodic laser wakefield. Different from the bubble regime, the main limitation on the energy gain comes here from the dephasing. The velocity of relativistic electrons is slightly higher than the phase velocity of the wake, which is determined by the group velocity of the driving laser pulse. The accelerated electrons slowly outrun the plasma wave and leave the accelerating phase.

The limitation caused by the dephasing can be overcome by employing a proper plasma gradient [18,32]. The profile of the plasma density should be such that the advance of the accelerated electrons matches the advance of the plasma wave. The equation for plasma density profile in the 1D configuration is, [32],

$$\frac{\mathrm{d}}{\mathrm{d}x}\left(\frac{\Phi}{\omega_p(x)}\right) \simeq 1 - \frac{c}{v_{gr}} \tag{3}$$

where $\omega_p(x) = \sqrt{4\pi e^2 n(x)/m}$ is the coordinate-dependent plasma frequency, Φ is the phase of ultrarelativistic electrons trapped in the plasma wake, v_{gr} is the group velocity of the laser pulse, c is the speed of light, e and m are the electron charge and mass, respectively. For weakly relativistic laser pulses with $a = eA/mc^2 \ll 1$ and for rarefied plasmas $n/n_c \ll 1$ we can assume $v_{gr}/c \simeq 1 - n(x)/2n_c$ and $\gamma \gg \gamma_{gr}$, where γ is the relativistic gamma-factor of the

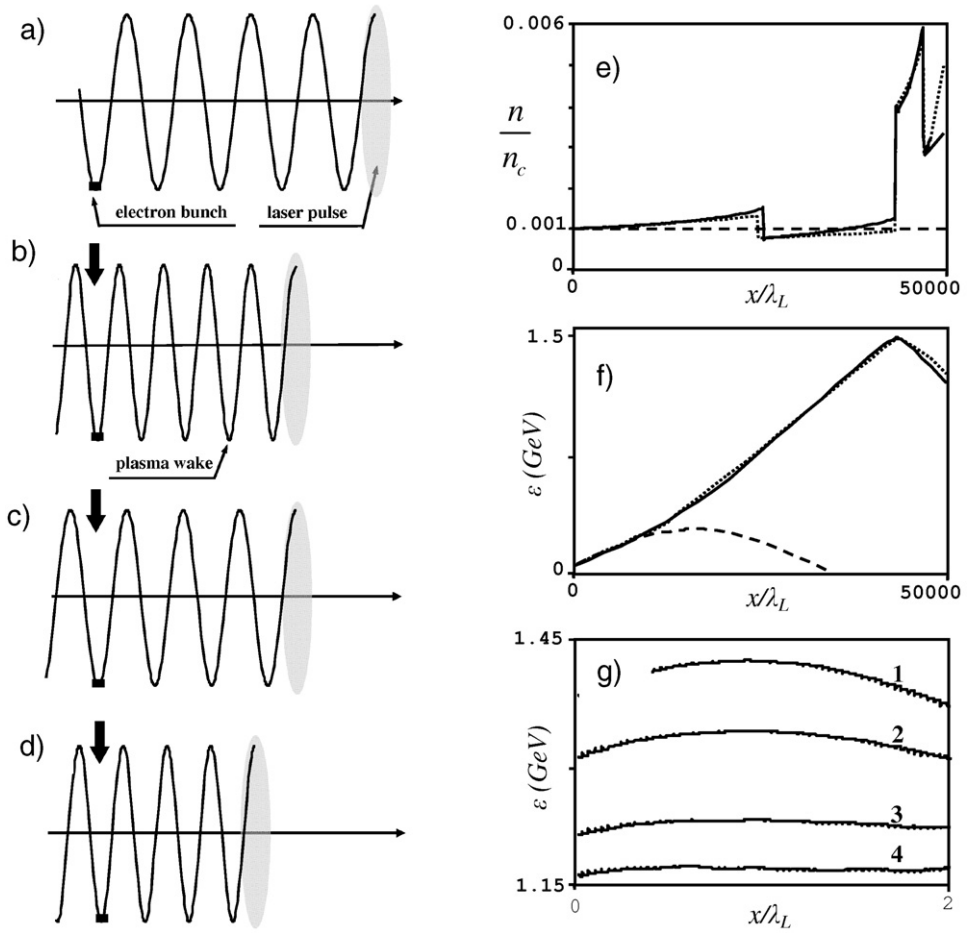

Fig. 4. (a)–(d): Schematics of electron acceleration in plasma layers in the frame of light speed. The ultra-relativistic electron bunch (black rectangle) is always located at the peak value of the accelerating field. (e)–(g): Simulations of electron bunch acceleration and energy spread reduction in plasma layers: (e) the plasma density profile, (f) the mean energy of the electron bunch, (g) electron energy vs electron position in the bunch. Electrons are accelerated by the first laser pulse in the first two layers ($0 < x < 43370\lambda_L$) whereas they are decelerated in the third and fourth layers ($43370\lambda_L < x < 49820\lambda_L$). The solid line and the dotted lines correspond to the PIC simulation results and the theoretical estimates, respectively. To compare, the dashed line shows acceleration in homogeneous plasma with the constant density $n_0 = 0.001 n_c$. The energy distributions in frame (g) are shown at the beginning of the deceleration at $x = 43370\ \lambda_L$ (line 1), at $x = 45370\ \lambda_L$ (line 2), at $x = 47370\ \lambda_L$ (line 3) and the end of deceleration at $x = 49820\ \lambda_L$ (line 4), respectively. The laser pulses are circularly polarized with Gaussian profile and wavelength 1 μm. The laser pulse parameters are $T = 10.6\lambda_L/c$, $a_0 = 0.6$ for the pulse on the acceleration stage and $T = 5.3\lambda_L/c$, $a_0 = 0.5$ for the pulse on the deceleration stage.

accelerated electrons, $\gamma_{gr}^{-2} = 1 - v_{gr}^2/c^2$, $n_c = m\omega^2/4\pi e^2$ is the critical plasma density and ω is the laser frequency. The solution of Eq. (3) providing $\Phi = \text{const}$ for the phase synchronism in laser wake field acceleration is

$$n(x) = \frac{n_0}{(1 - x/L_{inh})^{2/3}} \tag{4}$$

$$L_{inh} = \frac{c}{\omega}\left(\frac{n_0}{n_c}\right)^{-3/2}\frac{2\Phi}{3} \tag{5}$$

where $n_0 = n(x = 0)$. It follows from Eq. (4) that the plasma density increases along the pulse propagation and the acceleration distance is limited by L_{inh} since the plasma density goes to infinity at $x = L_{inh}$.

The acceleration length in the plasma density profile is limited by L_{inh} that also limits the electron energy gain.

In contrast to the acceleration scheme discussed by other authors [32,33], we have proposed a layered profile of the plasma density [18]. The layered plasma allows for a manifold increase in the acceleration efficiency. The acceleration

scheme [18] is illustrated in Figs. 4(a)–4(d). Let the electrons be trapped in the ith plasma period during acceleration in the first plasma layer where the plasma density increases from n_1 to some final value n_f in accordance with Eq. (4). The wake phase is synchronized to the electron bunch in this plasma layer due to the plasma density gradient. The wake phase at the electron bunch center is $\Phi_i = \pi(2i-1)$ that corresponds to the maximum of the accelerating force. When the plasma density reaches the value of n_f, the electron bunch enters the second plasma layer where the plasma density increases from n_2 to n_f. The density value of $n_2 = n_f \Phi_{i-1}^2/\Phi_i^2$ is chosen such that the electrons in the second layer become located in the $(i-1)$th plasma period behind the laser pulse. The wake phase at the electron bunch center is $\Phi_{i-1} = \pi(2i-3)$ that again corresponds to the maximum of the accelerating force. Inductively, the plasma density increases from $n_j = n_f \Phi_{i-j}^2/\Phi_{i-j-1}^2$ to n_f in the jth plasma layer in accordance with Eq. (4) and the electrons are trapped in the $(i-j)$th plasma period behind the laser pulse.

The successive acceleration in the several plasma layers by *the same driving laser pulse* leads to a much higher electron energy gain as well as the laser energy conversion efficiency than in the acceleration schemes discussed previously [32,33]. The transition region between plasma layers cannot be too short because of wave breaking and cannot be too long because the alternating force acting on electrons from the plasma wake may cause bunch heating and defocusing.

Further, the proposed scheme allows us to control the energy spectrum of the bunch electrons [18]. Naturally, electrons located at the bunch center get the greatest energy gain while electrons located at the bunch edges get the smallest energy gain. This leads to an energy spread of the bunch after the acceleration stage. To reduce this spread we suggest using a matched decelerating stage with a higher plasma density. Although the decelerating stage will reduce the net energy gain, its effect on the energy spread reduction is much stronger, because the plasma wake period decreases as the plasma density increases.

In order to check the validity of our simplified model, we have performed 1D PIC simulations, using the code Virtual Laser Plasma Laboratory [34]. The code has been supplemented with an adaptive scheme: the plasma density is varied in each time step so that the bunch center is always located in the maximal value of the accelerating force. The plasma wake excited by the first laser pulse in the first two layers accelerates the electron bunches while the bunch is decelerated in the second two layers where the plasma wake excited by the second pulse (see Fig. 4(e)). The laser pulses are circularly polarized with a Gaussian profile. The laser wavelength $\lambda_L = 1$ μm.

The duration of the first pulse is $T = 10.6\lambda_L/c$ and $a_0 = 0.6$ while the duration of the second pulse is $T = 5.3\lambda_L/c$ and $a_0 = 0.5$. The plasma density at the beginning of acceleration is $n_0 = 0.001 n_c$. The bunch center in the first layer is located at 3.5 plasma periods behind the pulse center (phase of bunch center is $\Phi_1 = -7\pi$). The second layer is chosen such that the bunch is located at 2.5 plasma periods behind the pulse center ($\Phi_2 = -5\pi$) there. For the decelerating layers $\Phi_3 = -8\pi$ and $\Phi_4 = -6\pi$ in the third and fourth layers. The electron bunch was initially monoenergetic with energy 50 MeV and duration $T_b = 2\lambda_L/c$.

The bunch energy achieves about 1.4 GeV with the energy spread of about 2% after acceleration in the first two plasma layers (see Figs. 4(f), 4(g)). On the deceleration stage, the bunch energy reduces to 1.2 GeV whereas the energy spread reduces to less than 0.5% (see Figs. 4(f), 4(g)). The total distance of the bunch acceleration and conditioning is about 5 cm. It is seen from Figs. 4(e), 4(f) that the plasma density profile and the bunch energy evolution obtained in PIC simulation agree fairly good with the theoretical prediction (4). To achieve a better agreement we take into account the pulse compression in the second half of the first layer (we suppose that $a_0 = 0.7$ and $T = 7.8\lambda_L/c$), in the second layer ($a_0 = 0.8$ and $T = 5.9\lambda_L/c$) and in the fourth layer ($a_0 = 0.6$ and $T = 3.7\lambda_L/c$) in accordance with PIC simulation results. The deviation of the numerical results from theoretical estimates is caused by the complex nonlinear dynamics of the laser pulse during propagation. According to Fig. 4(f), the energy gain in the inhomogeneous plasma is about 5 times more than that in the homogeneous plasma with $n = n_0 = \text{const}$.

The approach reported above is one-dimensional and thus does not take into account transverse dynamics of the laser pulse and electrons. The laser pulse can be efficiently guided by plasma channels over many Rayleigh lengths [35]. More complicated can be the transverse dynamics of accelerated electrons. It is well known [36] that the simultaneous accelerating and focusing of electrons occurs over a quarter of the plasma wavelength. Another accelerating quarter of the plasma wave defocuses electrons. At the maximum of the accelerating fields, however, the transverse fields vanish. The use of a preformed plasma channel can significantly extend the region where the accelerating and focusing phases overlap [37].

7. Conclusions

The physics of strong field laser–matter interaction is a dynamically developing field. In this article, we focused on the problem of quasi-monoenergetic electron acceleration in the Bubble regime as well as in periodic weakly relativistic wakes. In both cases, the effective phase velocity of the accelerating structures plays the most important role defining the quality of the produced electron beams. In the Bubble regime, it is the effective phase velocity that fluctuates during the propagation and influences the electron trapping process. In the weakly relativistic regime, one can manipulate the phase velocity by tapering the plasma density. This not only affects the dephasing, but also gives an opportunity to control the beam quality.

Acknowledgements

This work was supported by Transregio 18 project of DFG (Germany) and Russian Foundation for Basic Research (No 07-02-01239-a).

References

[1] M.D. Perry, G. Mourou, Physics Today 51 (1998) 228.
[2] M.H. Key, M.D. Cable, T.E. Cowan, et al., Phys. Plasmas 5 (1998) 1966.
[3] G.A. Mourou, D. Umstadter, Sci. Am. 286 (2002) 80.
[4] T. Tajima, J. Dawson, Phys. Rev. Lett. 43 (1979) 267.
[5] A. Pukhov, et al., Phys. Plasmas 6 (1999) 2847.
[6] A. Pukhov, J. Meyer-ter-Vehn, Appl. Phys. B 74 (2002) 355.
[7] S.P.D. Mangles, et al., Nature 431 (2004) 535.
[8] C.G.R. Gedder, et al., Nature 431 (2004) 538.
[9] J. Faure, et al., Nature 431 (2004) 541.
[10] W.P. Leemans, et al., Nat. Phys. 2 (2006) 418.
[11] J. Osterhoff, A. Popp, Z. Major, et al., Phys. Rev. Lett. 101 (2008) 085002.
[12] N.A.M. Hafz, T.M. Jeong, I.W. Choi, et al., Nat. Photonics 2 (2008) 571.
[13] I. Kostyukov, A. Pukhov, S. Kiselev, Phys. Plasmas 11 (2004) 5256.
[14] W. Lu, C. Huang, M. Zhou, W.B. Mori, T. Katsouleas, Phys. Rev. Lett. 96 (2006) 165002.
[15] S. Gordienko, A. Pukhov, Phys. Plasmas 12 (2005) 043109.
[16] A. Pukhov, S. Gordienko, Philos. Trans. R. Soc. A 364 (2006) 623.
[17] E. Esarey, et al., IEEE Trans. Plasma Sci. 24 (1996) 252.
[18] A. Pukhov, I. Kostyukov, Phys. Rev. E 77 (2008) 025401R.
[19] P. Sprangle, et al., Phys. Rev. Lett. 69 (1992) 2200.
[20] N.E. Andreev, et al., JETP. Lett. 55 (1992) 551.
[21] T.M. Antonsen, P. Mora, Phys. Rev. Lett. 69 (1992) 2204.
[22] E. Esarey, et al., Phys. Rev. Lett. 72 (1994) 2887.
[23] D. Umstadter, S.-Y. Chen, A. Maximchuk, G. Mourou, R. Wagner, Science 273 (1996) 472.
[24] E. Esarey, et al., Phys. Rev. Lett. 79 (1997) 2682.
[25] G. Shvets, N.J. Fisch, Phys. Rev. E 55 (1997) 6297.
[26] J. Faure, et al., Nature 444 (2006) 737.
[27] A.I. Akhieser, R.V. Polovin, JETP 3 (1956) 696.
[28] K.-C. Tzeng, et al., Phys. Plasmas 6 (1999) 2105.
[29] S.V. Bulanov, et al., Phys. Rev. Lett. 78 (1997) 4205.
[30] T.V. Liseikina, et al., Phys. Rev. E 60 (1999) 5991.
[31] J.K. Kim, D. Umstadter, in: Adv. Acc. Conc.: 8th Workshop, AIP Conf. Proc., vol. 472, AIP Press, NY, 1999, p. 404.
[32] T. Katsouleas, Phys. Rev. A 33 (1986) 2056.
[33] P. Sprangle, et al., Phys. Rev. Lett. 85 (2000) 5110.
[34] A. Pukhov, J. Plasma Phys. 61 (1999) 425.
[35] W.P. Leemans, et al., IEEE Trans. Plasma Sci. 24 (1996) 331.
[36] F.F. Chen, Laser accelerators, in: M.N. Rosenbluth, R.Z. Sagdeev (Eds.), Handbook of Plasma Physics, vol. 3, Elsevier Science Publishers B.V., Amsterdam, 1992, pp. 483–517.
[37] N.E. Andreev, et al., Phys. Plasmas 4 (1997) 1145.